VIA MEDICA

ORIGINAL ARTICLE

Folia Morphol.
Vol. 78, No. 1, pp. 124–136
DOI: 10.5603/FM.a2018.0063

ISSN 0015–5659
journals.viamedica.pl

The differential effects of high-fat and high--fructose diets on the liver of male albino rat and the proposed underlying mechanisms

S.M. Zaki[1, 2], S.A. Fattah[1], D.S. Hassan[1]

[1]*Department of Anatomy and Embryology, Faculty of Medicine, Cairo University, Cairo, Egypt*
[2]*Fakeeh College for Medical Sciences, Jeddah, Saudi Arabia*

[Received: 23 May 2108; Accepted: 26 June 2018]

Background: *The Western-style diet is characterised by the high intake of energy--dense foods. Consumption of either high-fructose diet or saturated fat resulted in the development of metabolic syndrome. Non-alcoholic fatty liver disease (NAFLD) is the hepatic manifestation of the metabolic syndrome. Many researchers studied the effect of high-fat diet (HFD), high-fructose diet (HFruD) and high-fructose high-fat diet (HFHF) on the liver. The missing data are the comparison effect of these groups i.e. are effects of the HFHF diet on the liver more pronounced? So, this study was designed to compare the metabolic and histopathological effect of the HFD, HFruD, and HFHF on the liver. The proposed underlying mechanisms involved in these changes were also studied.*

Materials and methods: *Twenty four rats were divided into four groups: control, HFD, HFruD, and HFHF. Food was offered for 6 weeks. Biochemical, light microscopic, immunohistochemical (Inducible nitric oxide synthase [iNOS] and alpha-smooth muscle actin [α-SMA]), real-time polymerase chain reaction (gene expression of TNF-α, interleukin-6, Bax, BCL-2, and caspase 3), histomorphometric analysis and oxidative/antioxidative markers (thiobarbituric acid reactive substances [TBARS], malondialdehyde [MDA]/glutathione [GSH] and superoxide dismutase [SOD]) were done.*

Results: *The HFD, HFruD and HFHF groups developed a cluster of liver disorders; steatosis, necrosis, inflammation, apoptosis, ballooning degeneration and cytoplasmic vacuolations. Internal metabolic impairments include elevated serum levels of glucose, triglycerides, low density lipoprotein and decreased serum levels of high density lipoprotein and albumin. The immunoreaction of the α-SMA and iNOS was strong in these groups. The oxidant markers (MDA and TBARS) were elevated, while the antioxidant markers (SOD and GSH) were decreased. The area per cent of collagen, inflammatory markers, caspase 3 and Bax were elevated, while the BCL-2/Bax ratio was decreased. The decrease in PAS, antioxidant markers and the elevation of the α-SMA, iNOS, inflammatory and oxidant markers were obvious in the HFHF when compared to that of the other groups.*

Conclusions: *High-fat diet, HFruD, and HFHF developed morphologic hepatic changes ranging from steatosis to necrosis and inflammation, besides the development of internal metabolic impairments. The chief factors of hepatic injury were fat accumulation in the hepatocytes, oxidative stress and highly elevated iNOS. Compared to the other groups, HFHF's effect was more prominent.* (Folia Morphol 2019; 78, 1: 124–136)

Key words: high-fat diet, high-fructose diet, high fructose high-fat diet, liver

Address for correspondence: Dr. S.M. Zaki, Fakeeh College for Medical Sciences, Jeddah, Saudi Arabia, e-mail: zakysherif1@gmail.com

INTRODUCTION

The Western-style diet is characterised by the high intake of energy-dense foods [19]. High-fructose corn syrup and saturated fats are two chief elements in this diet [19]. Consumption of either these two elements resulted in the development of metabolic syndrome (MS), which includes: insulin insensitivity, higher circulating triglycerides (TG) and weight gain from increased body fat [6]. In addition, the nutrition above the packing capability of adipose tissue results in precipitation of TG in different organs, causing steatosis and even organ dysfunction [38]. Moreover, high consumption of carbohydrates with or without fats increases the risk of obesity and diabetes [25]. Non-alcoholic fatty liver disease (NAFLD) is the commonest sort of liver diseases in the Western countries [21]. It is the hepatic manifestation of the MS which represents the major cause of liver-related morbidity and mortality [3]. It has a large scale, starting from simple fatty liver and extending to non-alcoholic steatohepatitis (NASH) [20].

Understanding the mechanisms for NASH is the key to apply real preventive and/or treatment approaches against this disease. There are many proposed mechanisms such as oxidative stress, TG accumulation, inflammation and apoptosis [12, 13, 15, 33].

The worldwide increments in the patient with MS have drawn the researchers' attention to introducing an experimental model that resembles the human [9]. Animal models fed with 40–60% high-fat diet develop insulin resistance, intrahepatic fat deposition, obesity and metabolic parameters close to human NASH [8].

Many researchers studied the effect of high-fat diet (HFD), high-fructose diet (HFruD) and high-fructose high-fat diet (HFHF) on the liver [21, 22, 39]. The missing data are the comparison effect of these groups i.e. are effects of the HFHF diet on the liver more pronounced? So, this study was designed to compare the metabolic and histopathological effect of the HFD, HFruD, and HFHF on the liver. The proposed underlying mechanisms involved in these changes were also studied.

MATERIALS AND METHODS

Twenty-four Sprague-Dawley adult male albino rats were acclimatised in the laboratory for a period of 2 weeks before carrying out the experiment. The rats were kept in cages at an ambient temperature of 26°C ± 2°C with 12 h light and 12 h dark cycle.

The animals were observed twice per day for signs of morbidity and mortality. The general toxicological data were recorded, including the motility, food and water consumption, health status and body weight gain.

The rats were divided into four equal groups (6 rats each):

— Control group: this group was given standard commercial diet (5.8% kcal of fat and 44.3% kcal carbs) [41];
— HFD group: this group was given ad lib water and high-fat chow which contained 60% kcal/g of fat, 20% kcal/g of carbohydrate from corn starch (Product #: D08060104, Research Diets, Inc., New Brunswick, NJ) [41];
— HFruD group: this group was given ad lib water and high-fructose chow which was 55% kcal/g of fructose, 10% kcal/g of fat (Product #: D05111802, Research Diets, Inc., New Brunswick, NJ) [41]. The rats were fed HFruD containing soybean oil to avoid the development of glucose intolerance [32];
— HFHF group: this group was given ad lib water and a diet containing 45% kcal/g of fat, 30% kcal/g of fructose [21].

Food and water were offered all the time for 6 weeks.

Body weight and food consumption measurements

Rats' body weight was measured at the beginning, then every week and just before sacrificing them. Their food consumption was measured on a daily basis.

The rats were sacrificed 24 h after the 6 weeks' experimental period. The liver specimens were excised and fixed in 70% alcohol, trimmed, washed, dehydrated in ascending grades of alcohol, cleared in xylol and processed for paraffin sections of 5 μm thickness.

Light microscopic study

Hematoxylin and eosin (H&E) stain

Masson's trichrome stain. For the demonstration of collagen fibres, the technique of Masson's trichrome stain was done according to Sheehan [30]. The paraffin sections were dewaxed, rehydrated then stained in acid fuchsin solution for 5 min, rinsed in distilled water, placed in phosphomolybdic acid solution for 3 min, washed in distilled water, stained with methyl blue solution for 2–5 min, rinsed in distilled water, and treated in acetic acid for 2 min. Finally, the

sections were dehydrated in absolute alcohol, cleared in xylol and mounted in Canada balsam. The nuclei appeared dark red, the cytoplasm appeared pale red and the collagen fibres appeared blue.

Histochemical evaluation (PAS stain)

The paraffin sections were dewaxed, rehydrated and then oxidised in 1% of periodic acid for 5 min. Then, they were washed with distilled water, treated with Schiff's reagent for 15 min, washed in running tap water for 5–10 min, counterstained in Harri's haematoxylin for 5 min, differentiated in 1% acid-alcohol, washed well in tap water, dehydrated in ascending grades of absolute alcohol, cleared in xylene, and mounted in Canada balsam. Glycogen and other reactive carbohydrates appeared magenta.

Analysis of the blood parameters

Blood samples were collected into serum-separating tubes at the end of the experiment, following a 12-h overnight fast. The samples were centrifuged at 3000 rpm for 15 min at 4°C. Serum was stored at –70°C until used in assays. Triglyceride (TG, mg/dL), cholesterol (mg/dL), high density lipoprotein (HDL, mmol/L); low density lipoprotein (LDL, (mmol/L), albumin (g/dL) and glucose (mmol/L) levels were determined using commercial kits (Asan Co. Ltd., Seoul, Korea).

Extraction and measurement of hepatic triglycerides

Total lipid was extracted from the liver by homogenizing with chloroform-methanol mixture (2:1, v/v) to a final dilution 20-fold the volume of the tissue sample [16]. The extraction was done in a tissue for 3 times. Pooled extract was dried using nitrogen evaporator. Hepatic TG were determined by colorimetric enzymatic assays [29].

Immunohistochemical study

The paraffin sections were dewaxed, rehydrated and incubated with 3% hydrogen peroxide solution for 30 min and endogenous peroxidase activity was blocked. Then, heat mediated antigen retrieval was performed and a microwave was utilised for tissue antigen retrieval. The sections were cleaned and put into phosphate buffered saline (PBS) for 5 min. After PBS was wiped off, the appropriate amount of serum was added to the sections at room temperature for 30 min. All techniques were done according to the manufacturer's instructions.

Inducible nitric oxide synthase. The sections from each paraffin block were incubated with a reaction buffer containing primary antibody anti inducible nitric oxide synthase (iNOS) antibody (ab15323 at a dilution of 1:100) for at least 14 h at 4°C. Afterward, the sections were incubated with Goat anti-Rabbit IgG H&L (HRP) (ab205718) for 20 min at 37°C. Each step was followed by adequately washing with PBS.

Alpha-smooth muscle actin. The alpha-smooth muscle actin (α-SMA) was performed to evaluate the degree of fibrosis [4]. The sections from each paraffin block were incubated with a reaction buffer containing primary antibody α-SMA antibody {(1A4) (ab7817) 1:100}. Afterward, the sections were incubated with Goat anti-Rabbit IgG H&L (HRP) (ab205718) for 20 min at 37°C. Each step was followed by adequately washing with PBS.

Oxidative/antioxidative markers in liver homogenates

Oxidative stress markers. Thiobarbituric acid reactive substances (TBARS) and malondialdehyde (MDA) were measured according to Tipple and Rogers [36]. This method measures the colour produced by the reaction of the thiobarbituric acid (TBA) with lipid peroxides, TBARS at 532 nm. 100 mg of tissue was homogenised and precipitated with equal volume of 8.1% sodium dodecyl sulphate, 20% acetic acid solution adjusted to pH 7.4 in 1 mL PBS. 0.8% TBA solution was added to the liver tissue homogenate to precipitate the protein and then centrifuged. Supernatants were collected and TBA solution was added to the supernatants. After boiling for 10 min in water bath, the absorbance was measured.

Anti-oxidative markers. Tissue glutathione (GSH) content was measured according to Tipple and Rogers [36]. The measurement of GSH is based on the reduction of 5, 5 dithiobis (2-nitrobenzoic acid) (DTNB) with reduced glutathione to produce a yellow compound. The reduced chromogen is directly proportional to GSH concentration and its absorbance is measured at 405 nm by using a commercial kit (Biodiagnostic, Egypt).

The superoxide dismutase (SOD) activity in liver homogenate was measured according to Weydert and Cullen [40] by the inhibition of nitroblue tetrazolium reduction by O_2-generated by the xanthine/xanthine oxidase system. One unit is the amount of SOD that inhibits the rate of formazan dye formation by 50%.

Table 1. The primers sequence for the studied genes

Isoform	Forward primer	Reverse primer
TNF-α	5′- TGAGATTCGTGCACAAGAGG-3′	5′- GTCATGGCTTTGGATGTCCT-3′
β-actin	5′-CTTTGATGTCACGCACGATTTC -3′	5′- GGGCCGCTCTAGGCACCAA-3′
IL-6	5′-GCCCTTCAGGAACAGCTATGA-3′	5′-CATCAGTCCAAGAAGGCAACT-3′
Caspase 3	5′-TTCAGAGGGGATCGTTGTAGAAGTC-3′	5′- CAAGCTTGTCGGCATACTGTTTCAG-3′
Bax	5′-CTGAGCTGACCTTGGAGC -3′	5′- GACTCCAGCCACAAAGATG-3′
BCL-2	5′-GACAGAAGATCATGCCGTCC -3′	5′- GGTACCAATGGCACTTCAAG-3′

TNF-α — tumour necrosis factor alpha; Il-6 — interleukin 6

Image analysis and morphometric measurements

The optical density of PAS and area per cent of collagen fibres and immune expression of iNOS and α-SMA were done using Leica LAS V3.8 image analyser computer system (Switzerland). The measurements were obtained by an independent blinded observer. The data was obtained in ten non-overlapping microscopic fields taken randomly from each slide and were examined within the standard measuring frame, using a magnification of ×400. Within the measuring frame, the area per cent were detected and masked by a binary colour.

Real-time polymerase chain reaction (PCR) (gene expression of TNF-α, IL-6, Bax, BCL-2, and caspase 3)

Total RNA extraction. Total RNA was extracted from the thyroid tissue using the TRIzol method according to the manufacturer's protocol (Invitrogen, Life Technologies, Waltham, MA, USA). In brief, RNA was extracted by homogenisation in a TRIzol reagent. The homogenate was then incubated for 5 min at room temperature. A 1:5 volume of chloroform was added, and the tube was vortexed and centrifuged at 12,000 g for 15 min. Thereafter, the aqueous phase was isolated, and the total RNA was precipitated with absolute ethanol. After centrifugation and washing, the total RNA was finally diluted in 20 μL of the RNase-free water. The RNA concentrations and purity were measured with an ultraviolet spectrophotometer at 260 nm.

Complementary DNA (cDNA) synthesis. The cDNA was synthesized from 1 μg RNA using Superscript III First-Strand Synthesis; a system as described in the manufacturer's protocol (Invitrogen, Life Technologies). In brief, 1 μg of total RNA was mixed with 50 μM oligo (DT) 20, 50 ng/μL random primers, and 10 mM dNTP mix in a total volume of 10 μL. The mixture was incubated at 56°C for 5 min and then placed on ice for 3 min.

The reverse transcriptase master mix containing 2 μL of 10× RT buffer, 4 μL of 25 mM MgCl2, 2 μL of 0.1 M DTT, and 1 μL of SuperScript® III RT (200 U/μL) was added to the mixture and was incubated at 25°C for 10 min followed by 50 min at 50°C.

Real-time quantitative PCR. The relative abundance of mRNA species was assessed using the SYBR Green method on an ABI prism 7500 sequence detector system (Applied Biosystems, Foster City, CA, USA). PCR primers were designed with Gene Runner Software (Hasting Software, Inc., Hasting, NY, USA) from RNA sequences from Gen Bank. All primer sets had a calculated annealing temperature of 60°. Real-time quantitative PCR was performed in a 25-μL reaction volume consisting of 2X SYBR Green PCR Master Mix (Applied Biosystems), 900 nM of each primer and 2–3 μL of cDNA. Amplification conditions were 2 min at 50°, 10 min at 95° and 40 cycles of denaturation for 15 s and annealing/extension at 60° for 10 min. Data from RT assays were calculated using the v1·7 Sequence Detection Software from PE Biosystems (Foster City, CA). Relative expression of studied gene mRNA was calculated using the comparative Ct method. All values were normalised to the β-actin gene and reported as fold change (Table 1).

Statistical analysis

Statistical analysis was performed using statistical package for the social sciences statistical software (SPSS) version 21.0 (IBM Corporation, Somers, NY, USA). The data were expressed as means ± standard deviation (SD). Statistical evaluation was done using one-way analysis of variance (ANOVA) followed by Bonferroni pairwise comparisons. Significance was considered when the p-value was ≤ 0.05. The percentage of increase or decrease (difference) in all study parameters

were calculated per the following formula: Percentage of difference = (mean difference value between two groups) / (value of the compared group) × 100.

RESULTS

The general toxicological data (Table 2)

No mortalities were observed in all studied groups. The motility, food and water consumption and health status were relatively good.

The body weight at the beginning of the study was 149.0 ± 3.6 g. At the end of the study, the animals of all studied groups gained weight; their mean body weights increased by 15%, 24.7%, and 23.5% in the HFD, HFruD and HFHF groups as compared to that of the control group. A non-significant difference was observed in the HFD, HFruD and HFHF groups when compared to each other.

Table 2. The mean of the body weight (BW) gain in the different experimental groups

Group	BW	Versus group	P
Control	170.0 ± 5.0		
HFD	200.7 ± 10.1	Control	0.044*
		HFruD	1.000
		HFHF	1.000
HFruD	212.0 ± 4.0	Control	0.007*
		HFD	1.000
		HFHF	1.000
HFHF	210.0 ± 17.3	Control	0.010*
		HFD	1.000
		HFruD	1.000

Data are shown as mean ± standard deviation.
The body weight at the beginning of the study was 149.0 ± 3.6 g.
*p-value significant; other abbreviations — see text

The general structure of the liver as shown by H&E staining

The liver of the control group exhibited the normal histological architecture around the central vein (Fig. 1A). The HFD, HFruD and HFHF groups exhibited different forms of hepatic necrosis: pyknosis, karyorrhexis, and karyolysis. Hepatocytes with apoptosis, steatosis (microvesicular and macrovesicular) and cytoplasmic vacuolations were also detected in these groups. Hepatocytes with ballooning degeneration were only identified in the HFD and HFHF groups (Fig. 1B–E).

The portal area of the control rat was presented with the normal histological pattern (Fig. 2A). The portal veins of the three experimental Western diet groups were dilated and congested with interrupted endothelium. Inflammatory cellular infiltrations with steatosis (microvesicular and macrovesicular) around the periportal areas were also realized in these groups (Fig. 2B–D).

The content of collagen fibres

The collagen fibres around the periportal area were minimum in the control group (Fig. 3A). Collagen tissue fibres increased by 310% (3 folds), 306% (3 folds) and 229% (2 folds) in the HFD, HFruD and HFHF groups when compared to that of the control group (Fig. 3B–D, Table 3). Non-significant differences were observed between the HFD, HFruD and HFHF groups when compared to each other.

Histochemical evaluation (PAS stain)

A strong PAS reaction was observed in the control group (Fig. 4A). The reaction displayed 36%, 48%, and 60% significant decrease when compared to that of the control group. The decrease in the HFHF group was 47% and 30.7% compared to that of the HFD, HFruD groups (Fig. 4B–D, Table 3).

Immunohistochemical evaluation

The reaction of the α-SMA was slight in the control group (Fig. 5A). When comparing the HFD, HFruD and HFHF groups with the control group, there were significant elevations in the mean area per cent of the α-SMA by 433% (4 folds), 173% (1.7 folds) and 750% (7.5 folds), respectively. The elevation in the HFHF group was 56% and 210% compared to that of the HFD, HFruD groups (Fig. 5B–D, Table 3).

The iNOS reaction was absent in the control group (Fig. 6A). Such reaction presented high elevation in the HFD, HFruD and HFHF groups by 767% (7.6 folds), 903% (9 folds) and 1458% (14 folds), respectively when compared to that of the control group. The elevation in the HFHF group was 84.6% and 255% compared to that of the HFD, HFruD groups (Fig. 6B–D, Table 3).

Biochemical evaluation (Table 4)

Regarding the hepatic TG, there was a significant rise in their mean values by 83%, 50% and 112% in the HFD, HFruD and HFHF groups, respectively compared to that of the control group.

The mean values of the serum TG in the HFD, HFruD and HFHF groups revealed 59%, 40%, and 76% significant increase, respectively, when compared to that of the control group. At the same time, the mean

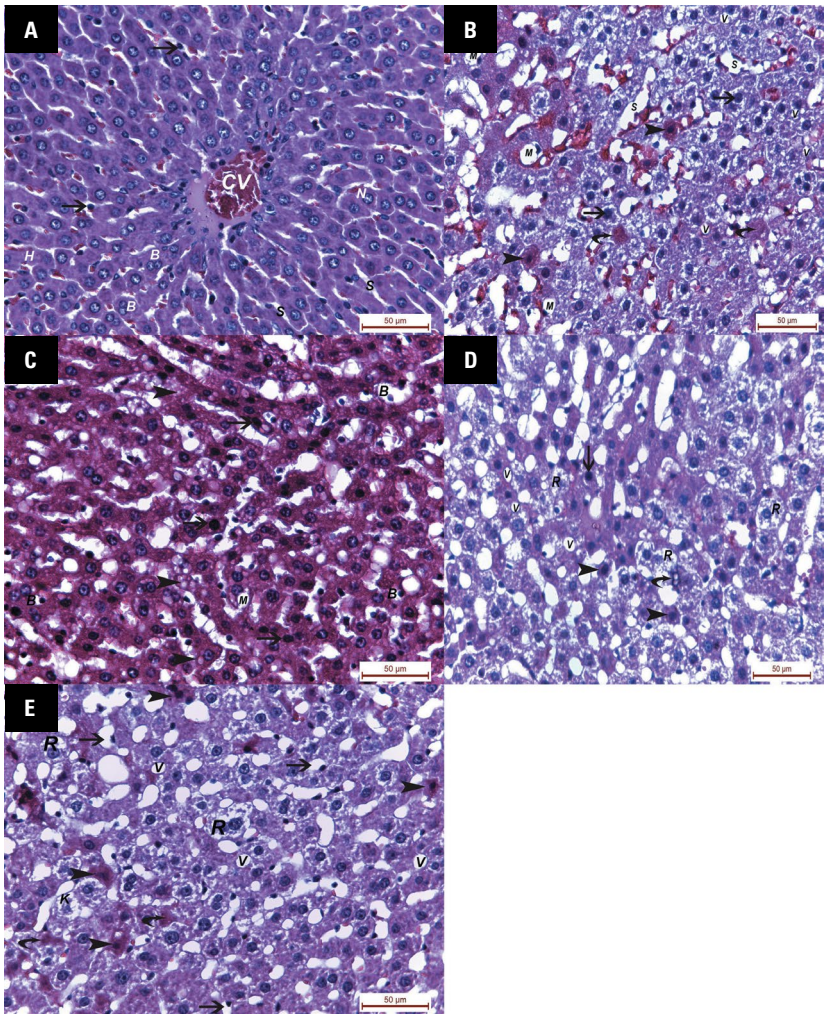

Figure 1. Liver sections around central veins in different groups; **A.** Central vein (CV) and sinusoids (S) with Von-Kupffer cells (arrows). The hepatocytes (H) and nuclei (N) with central nucleolus. Some hepatocytes are binucleated (B) in a rat of the control group; **B.** Hepatocytes with apoptosis (arrowheads) and hepatocytes with ballooning degeneration (M). Nuclear necrosis in the form of pyknosis (arrows) and karyolysis (curved arrows). Note dilated sinusoids (S) and microvesicular steatosis (V) in a rat of the high-fat diet group; **C.** Hepatocytes with pyknotic nuclei (arrows) and with ballooning degeneration (B). Note microvesicular steatosis (arrowheads) and macrovesicular steatosis (M) in a rat of the high-fat diet group; **D.** Hepatocytes with apoptosis (arrowheads) and degenerated hepatocytes with rarefied cytoplasm (R) in a rat of the HFruD group. Note pyknosis (arrows) and signet ring nuclei (curved arrow) with intrahepatic vacuolations (V); **E.** Hepatocytes with rarefied cytoplasm (R), apoptosis (arrowheads), karyolysis (curved arrows) and karyorrhexis (k). Note ballooning hepatic degeneration (arrows) and microvesicular steatosis (V) in a rat of the HFHF group. Haematoxylin and eosin staining. Scale bars = 50 μm, total magnification $\times$400.

values of the cholesterol of the HFD, HFruD and HFHF groups showed 58%, 42%, and 87% significant rise, when compared to that of the control group.

On the other hand, the mean levels of HDL in the HFD, HFruD and HFHF groups was significantly decreased by 59%, 47%, and 59%, compared to that of the control group.

The mean LDL values in the HFD, HFruD and HFHF groups displayed 180%, 135% and 238% significant upsurge respectively when compared to that of the control group.

When comparing the HFD, HFruD and HFHF groups with the control group, there was a significant decrease in the mean values of albumin (by 29%, 20%, and 45%, respectively) and a significant increase in the mean glucose level (by 85%, 105%, and 122%, respectively).

Inflammatory and oxidative/antioxidative markers' evaluation (Table 5)

The mean values of the tumour necrosis factor alpha (TNF-α) in the HFD, HFruD and HFHF groups were 126% (1.26 folds), 190% (1.9 folds) and 229% (2.29 folds) higher than in the control group. The elevation in the HFHF group was 45.6% and 13.2% compared to that of the HFD, HFruD groups.

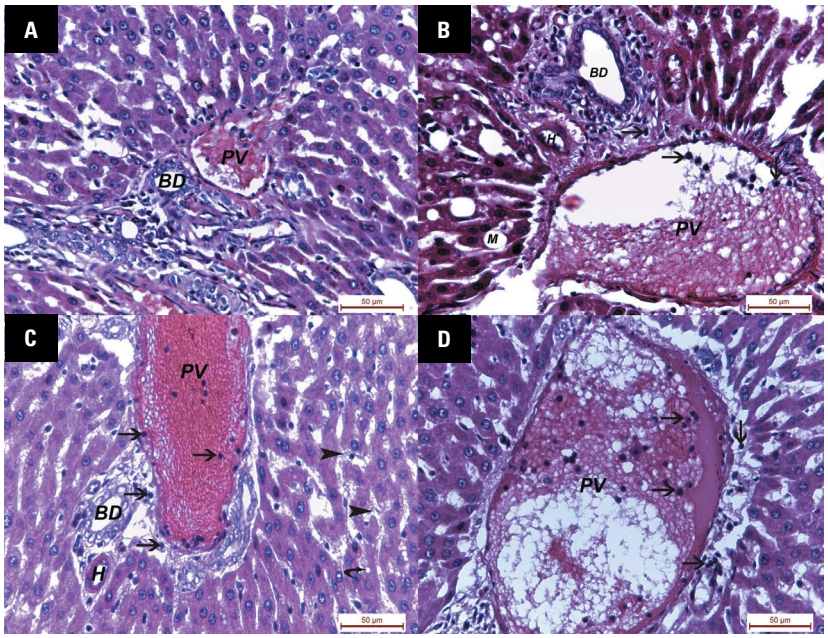

Figure 2. Liver sections around the portal area in different groups. Note: portal vein radicle (PV), hepatic artery (H) and bile ductule (BD) lined with cuboidal epithelium; **A.** A rat of the control group; **B.** Dilated congested portal vein (PV) with interrupted endothelium, inflammatory cellular infiltrations (arrows), microvesicular steatosis (curved arrows) and macrovesicular steatosis (M) in a rat of the high-fat diet group; **C.** A dilated congested portal vein (PV), inflammatory cellular infiltrations (arrows), microvesicular steatosis (curved arrows) and apoptosis (arrowheads) in a rat of the HFruD group; **D.** A dilated portal vein (PV), inflammatory cellular infiltrations (arrows) and apoptosis (arrowhead) in a rat of the HFHF group. Haematoxylin and eosin staining. Scale bars = 50 μm, total magnification ×400.

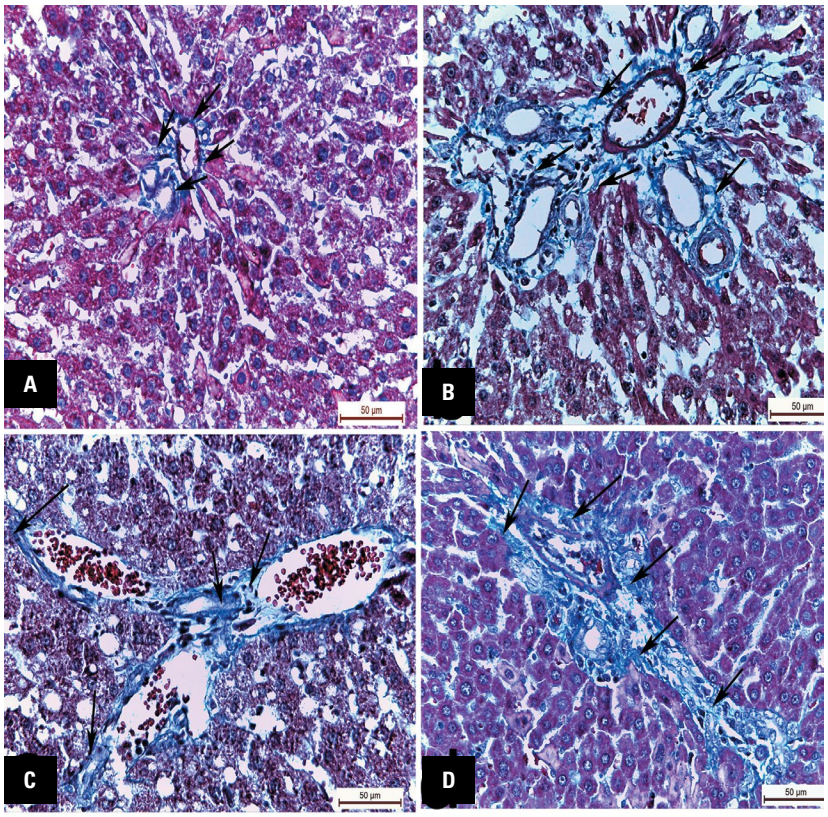

Figure 3. Collagen fibres (arrows) around the periportal area in different groups; **A.** Minimal amount of collagen fibres in the control group; **B–D.** Increased amount of collagen fibres in the HFD, HFruD and HFHF groups, respectively. Masson's trichrome staining. Scale bars = 50 μm, total magnification ×400.

Table 3. Area per cent of collagen fibres, inducible nitric oxide synthase (iNOS), alpha-smooth muscle actin (α-SMA) and optical density of periodic acid-Schiff (PAS) among the different groups

Group		Area per cent of collagen	PAS optical density	α-SMA	iNOS
Control	Mean ± SD	**1.47 ± 0.64**	**0.26 ± 0.01**	**3.0 ± 1.0**	**3.1 ± 0.8**
HFD	Mean ± SD	**6.03 ± 0.45**	**0.17 ± 0.04**	**16.0 ± 1.9**	**26.0 ± 2.0**
	Versus control	0.000*	0.000*	0.000*	0.000*
	Versus HFruD	1.000	0.007*	0.005*	0.027*
	Versus HFHF	0.315	0.000*	0.001*	0.000*
HFruD	Mean ± SD	**5.97 ± 0.68**	**0.13 ± 0.02**	**8.2 ± 1.7**	**31.1 ± 1.7**
	Versus control	0.000*	0.000*	0.054	0.000*
	Versus HFD	1.000	0.007*	0.005*	0.027*
	Versus HFHF	0.385	0.007*	0.000*	0.000*
HFHF	Mean ± SD	**4.85 ± 0.73**	**0.09 ± 0.01**	**25.5 ± 2.5**	**48.3 ± 1.7**
	Versus control	0.001*	0.000*	0.000*	0.000*
	Versus HFD	0.315	0.007*	0.001*	0.000*
	Versus HFruD	0.385	0.000*	0.000*	0.000*

*p-value significant; SD — standard deviation; other abbreviations — see text

Table 4. Biochemical parameters of the studied groups

Group		Hepatic TG [μmmol/gprot]	Serum TG [mg/dL]	TC [mg/dL]	HDL-C [mmol/L]	LDL-C [mmol/L]	Albumin [g/dL]	Glucose [mmol/L]
Control	Mean ± SD	**49.3± 3.1**	**68.7 ± 4.2**	**131.7 ± 3.1**	**61.0 ± 2.0**	**57.3 ± 3.9**	**5.5 ± 0.3**	**89.0 ± 11.8**
HFD	Mean ± SD	**90.0 ± 5.0**	**108.7 ± 7.6**	**208.3 ± 17.2**	**25.3 ± 9.3**	**160.7 ± 7.3**	**3.9 ± 0.7**	**165.0 ± 9.2**
	Versus control	0.000*	0.000*	0.000*	0.000*	0.000*	0.01*	0.000*
	Versus HFruD	0.007*	0.183	0.162	1.000	0.011*	1.000	0.197
	Versus HFHF	0.014*	0.227	0.008	1.000	0.002*	0.211	0.008*
HFruD	Mean ± SD	**74.0 ± 3.6**	**96.0 ± 6.6**	**187.0 ± 7.8**	**32.3 ± 5.5**	**134.9 ± 4.3**	**4.4 ± 0.4**	**182.7 ± 6.8**
	Versus control	0.000*	0.003*	0.001*	0.002*	0.000*	0.06	0.000*
	Versus HFD	0.007*	0.183	0.162	1.000	0.011*	1.000	0.197
	Versus HFHF	0.000*	0.006*	0.000	0.978	0.000*	0.036*	0.335
HFHF	Mean ± SD	**104.3 ± 4.0**	**120.7 ± 4.7**	**246.3 ± 2.5**	**25.0 ± 4.0**	**193.9 ± 10.3**	**3.0 ± 0.1**	**198.0 ± 3.6**
	Versus control	0.000*	0.000*	0.000*	0.000*	0.000*	0.001*	0.000*
	Versus HFD	0.014*	0.227	0.008	1.000	0.002*	0.211	0.008*
	Versus HFruD	0.000*	0.006*	0.000	0.978	0.000*	0.036*	0.335

*p-value significant; HDL-C — high density lipoprotein cholesterol; LDL-C — low density lipoprotein cholesterol; TC — total cholesterol; TG — triglyceride; SD — standard deviation; other abbreviations — see text

The mean values of the interleukin 6 (IL-6) in the HFD, HFruD and HFHF groups showed 230% (2.3 folds), 383% (3.83 folds) and 426% (4.26 folds) elevation, respectively, when compared to that of the control group. The elevation in the HFHF group was 59.3% when compared to that of the HFD group.

The mean levels of MDA in the HFD, HFruD and HFHF groups were significantly increased by 526% (5.26 folds), 746% (7.46 folds) and 1000% (10 folds) when compared to that of the control group. The increase in the HFHF group was 77.4% and 30.9% compared to that of the HFD, HFruD groups.

In addition, the mean values of TBARS were significantly increased by 122% (1.22 folds), 175% (1.75 folds) and 325% (2.29 folds), respectively, when compared to that of the control group. The increase in the HFHF group was 48.2% and 54.5% compared to that of the HFD, HFruD groups.

Table 5. Inflammatory and oxidative/antioxidative markers in the different studied groups

Group		TNF-α [g/mL]	IL-6 [g/mL]	MDA [nmol/mg protein]	TBARS [nmol/mg protein]	SOD [U/mg protein]	GSH [U/mg protein]
Control	Mean ± SD	**37.5 ± 5.3**	**18.7 ± 3.2**	**5.0 ± 2.0**	**20.0 ± 10.0**	**84.0 ± 5.3**	**144.0 ± 2.0**
HFD	Mean ± SD	**84.6 ± 12.2**	**61.7 ± 7.6**	**31.3 ± 3.2**	**44.3 ± 5.0**	**64.0 ± 3.6**	**95.0 ± 5.0**
	Versus control	0.000*	0.000*	0.000*	0.01*	0.005*	0.000*
	Versus HFruD	0.020*	0.001*	0.024*	0.504	0.007*	0.002*
	Versus HFHF	0.001*	0.000*	0.000*	0.000*	0.000*	0.000*
HFruD	Mean ± SD	**108.8 ± 4.7**	**90.3 ± 5.5**	**42.3 ± 2.5**	**55.0 ± 5.0**	**45.0 ± 5.0**	**74.7 ± 4.5**
	Versus control	0.000*	0.000*	0.000*	0.001*	0.000*	0.000*
	Versus HFD	0.020*	0.001*	0.024*	0.504	0.007*	0.002*
	Versus HFHF	0.236	0.571	0.011*	0.003*	0.005*	0.002*
HFHF	Mean ±SD	**123.2 ± 2.9**	**98.3 ± 2.9**	**55.0 ± 5.0**	**85.0 ± 5.0**	**25.0 ± 5.0**	**54.3 ± 4.0**
	Versus control	0.000*	0.000*	0.000*	0.000*	0.000*	0.000*
	Versus HFD	0.001*	0.000*	0.000*	0.000*	0.000*	0.000*
	Versus HFruD	0.236	0.571	0.011*	0.003*	0.005*	0.002*

*p-value significant; GSH — glutathione; Il-6 — interleukin 6; MDA — malondialdehyde; SD — standard deviation; SOD — superoxide dismutase; TBARS — thiobarbituric acid reactive substances; TNF-α — tumour necrosis factor alpha; other abbreviations — see text

Table 6. BCL-2, Bax, BCL-2/Bax ratio and caspase 3 among the different groups

Group		BCL-2	Bax	BCL-2/Bax ratio	Caspase 3
Control	Mean ± SD	**0.8 ± 0.2**	**0.25 ± 0.03**	**0.9 ± 0.1**	**1.3 ± 0.3**
HFD	Mean ± SD	**0.9 ± 0.1**	**1.4 ± 0.1**	**0.6 ± 0.0**	**3.0 ± 0.5**
	Versus control	1.000	0.003*	0.02*	0.006*
	Versus HFruD	1.000	0.099	1.000	1.000
	Versus HFHF	0.400	0.004*	1.000	0.095
HFruD	Mean ± SD	**1.0 ± 0.1**	**1.7 ± 0.2**	**0.6 ± 0.1**	**3.5 ± 0.4**
	Versus control	0.600	0.000*	0.01*	0.001*
	Versus HFD	1.000	0.099	1.000	1.000
	Versus HFHF	1.000	0.318	1.000	0.800
HFHF	Mean ± SD	**1.1 ± 0.1**	**1.9 ± 0.1**	**0.6 ± 0.1**	**4.0 ± 0.5**
	Versus control	0.100	0.000*	0.009*	0.000*
	Versus HFD	0.400	0.004*	1.000	0.095
	Versus HFruD	1.000	0.318	1.000	0.800

*p-value significant; SD — standard deviation; other abbreviations — see text

On the other hand, the mean levels of SOD in the HFD, HFruD and HFHF groups exhibited 24%, 46%, and 70% decrease compared to that of the control group. The decrease in the HFHF group was 60.9% and 44.4% compared to that of the HFD, HFruD groups.

In addition, the mean values of GSH decreased significantly by 34%, 48%, and 62%, respectively, compared to that of the control group. The decrease in the HFHF group was 43% and 27.3% compared to that of the HFD, HFruD groups.

BCL-2, Bax, BCL-2/Bax ratio and caspase 3 (Table 6)

Non-significant changes occurred in the BCL-2 among the different groups.

The mean value of the Bax in the HFD, HFruD and HFHF groups increased by 460% (4 folds), 580% (5 folds) and 660% (6 folds); while the mean values of the BCL-2/Bax ratio in these groups decreased by 33% when compared to that of the control group.

The mean value of the caspase 3 in the HFD, HFruD and HFHF groups increased by 130%, 169%, and 207% when compared to that of the control group.

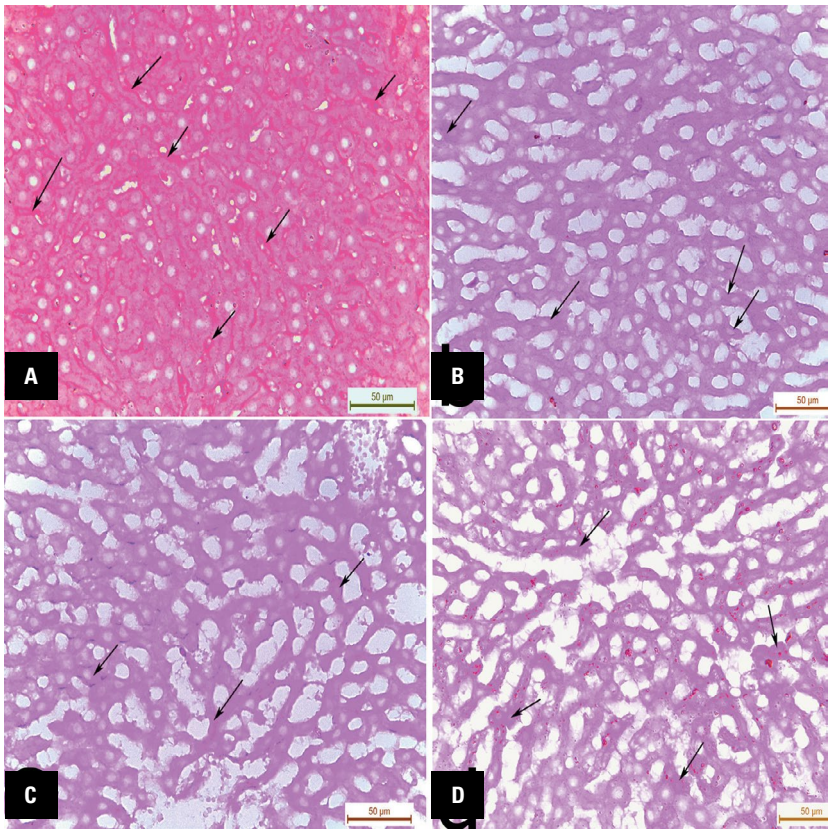

Figure 4. Liver sections showing the periodic acid-Schiff (PAS) reaction (arrows) in different groups; **A.** Strong PAS reaction in the control group; **B–D.** Decreased PAS reaction in the HFD, HFruD and HFHF groups, respectively. PAS staining. Scale bars = 50 μm, total magnification $\times$400.

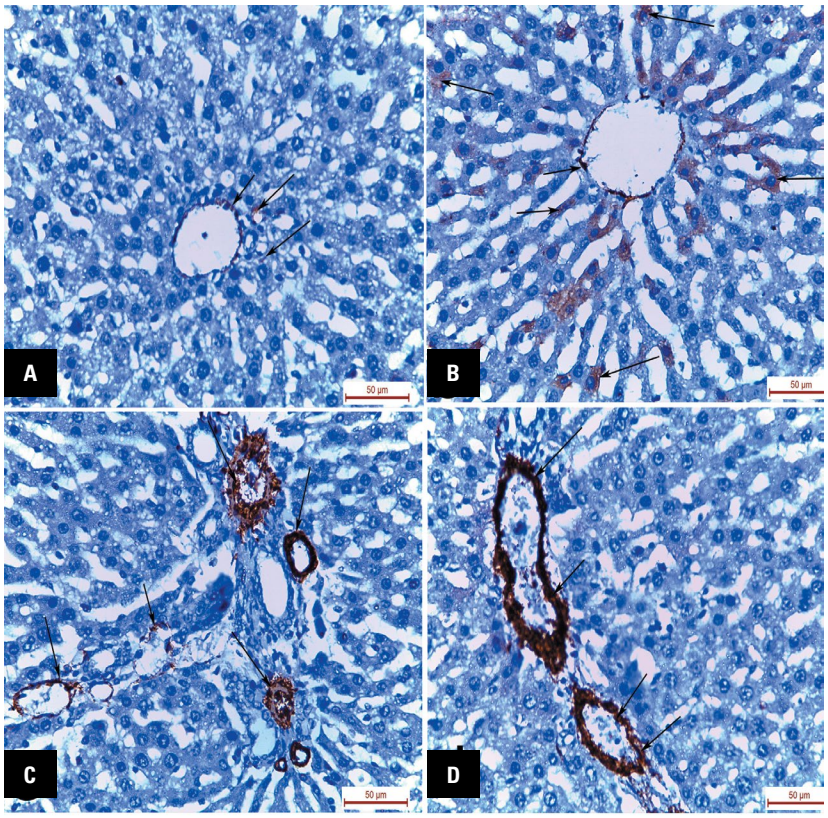

Figure 5. The immunoreaction of the and alpha-smooth muscle actin (α-SMA; arrows) in different groups; **A.** Slight reaction in the control group; **B–D.** Strong reaction in the HFD, HFruD and HFHF groups respectively. The immunohistochemical visualisation of α-SMA was performed as described in methods. Scale bars = 50 μm, total magnification $\times$400.

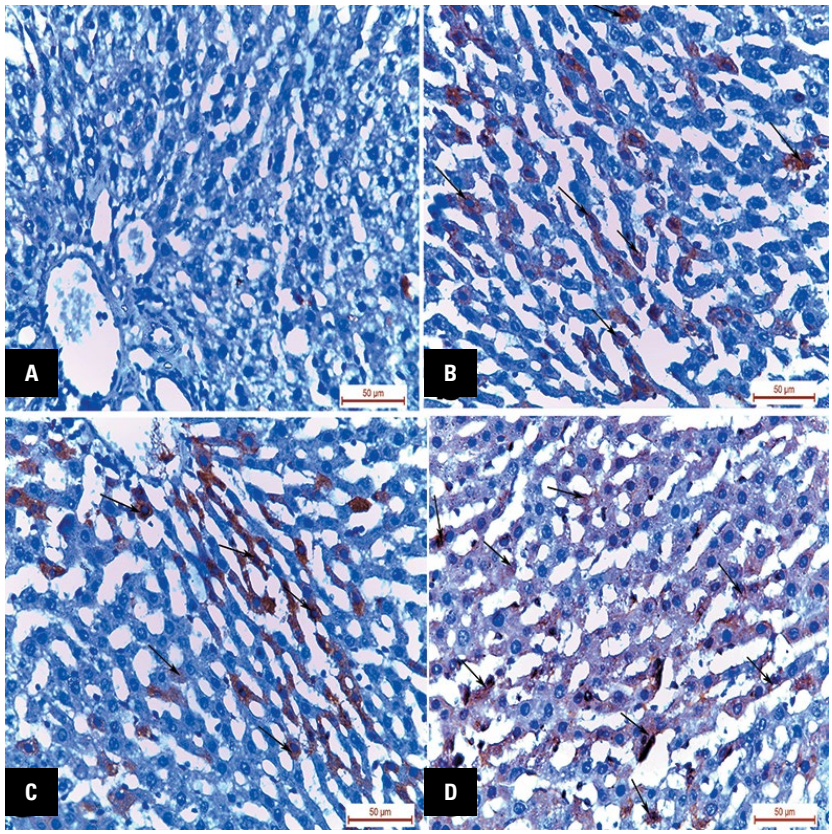

Figure 6. The immunoreaction of the inducible nitric oxide synthase (iNOS; arrows) in different groups (×400); **A.** No reaction in the control group; **B–D.** Strong reaction in the HFD, HFruD and HFHF groups respectively. The immunohistochemical visualisation of iNOS was performed as described in methods. Scale bars = 50 μm, total magnification ×400.

A non-significant difference of Bax, BCL-2/Bax and caspase 3 was observed in the HFD, HFruD and HFHF groups when compared to each other.

DISCUSSION

The HFD, HFruD and HFHF groups developed a significant increase in weight gain. Such weight gain is mostly due to the gradual accumulation in body fat [21]. Obesity is a key feature of the MS [2]. The HFD, HFruD and HFHF groups developed 'internal' metabolic impairments including elevated serum levels of albumin, glucose, TG, LDL. In addition, the level of HDL was decreased.

The HFD, HFruD and HFHF groups developed a cluster of liver disorders ranging from steatosis to necrosis and inflammation (NASH). All these features are named collectively NAFLD [3]. Observed only in the HFD and HFHF groups, ballooned hepatocytes are delimited to the most severe form of hepatic injury and indicate cell necrosis [7].

The chief factor of hepatic injury is lipid build-up in liver cells [7]. Fat accumulation in the liver plays a critical role in the initiation and progression of NAFLD [22].

The other major cause of hepatic injury is the oxidative stress [28]. Oxidative stress was developed in three Western diet groups being highest in the HFHF group. It is defined as the shift in the balance between oxidants and antioxidants in favour of oxidants [5, 6]. The oxidant markers (MDA and TBARS) were elevated, while the antioxidant markers (SOD and GSH) were decreased in all Western diet groups. The oxidative stress is mostly caused by the developed obesity [41]. In NAFLD progression, the "two-hit" theory is generally established [11]. The first hit is lipid accumulation in the hepatocytes and the second hit is oxidative stress-induced lipotoxicity, which stimulates cellular injury leading to NASH [26].

The other possible cause of hepatic injury is the elevation of the iNOS. The iNOS increased 7.6 folds in HFD group, 9 folds in HFruD and 14 folds in HFHF group. The NO-derived from iNOS appears to induce inflammation and oxidative stress [10]. These events create a deleterious environment that ultimately leads to cellular damages.

Steatosis observed in the Western diet groups may be due to the taken nutrition above the packing capability of adipose tissue which results in precip-

itation of TG in the liver [38]. Steatosis may be also correlated with the observed increased expression of iNOS in such groups [17].

Inflammation was observed around the periportal area. In addition, the TNF-α and IL-6 were elevated in the HFD, HFruD and HFHF groups being highest in the HFHF group. Obesity has been found to release these inflammatory cytokines from fat [14]. In addition, increased apoptosis could be an important mechanism leading to inflammation in the liver [39]. Fructose in the HFruD and HFHF groups facilitates the inflammation through the increase in the lipopolysaccharides influx from the gut [24]. Such increase induces intrahepatic innate immunity and ROS production [31]. In addition, fructose promotes the hepatic inflammation through augmented gut endotoxin-mediated Kupffer cells activation [18].

The area per cent of collagen fibres was elevated in the HFD, HFruD and HFHF groups being higher in the first two groups. Hepatic fibrosis is one of the main features of NASH [21] and represents the later stages of NAFLD [34]. The degree of TG deposition is predictive of the severity of the fibrosis [34]. The degree of fibrosis was evaluated by using the α-SMA [4]. The highest elevation was observed in the HFHF (7.5 folds), followed by the HFD group (4 folds), followed finally by the HFruD (1.7 folds).

Hepato-cellular apoptosis has been identified in the HFD, HFruD and HFHF groups. Apoptosis is a prominent feature of NASH [14, 27] and is a key component in the pathogenesis, development, and progression of the NASH [27]. The framework of the apoptotic signal pathway appears to be several pro-apoptotic signals which eventually converge into a common mechanism driven by caspases [35]. Caspase is a unique set of cysteine proteases that cleave critical cellular proteins [35]. Caspase 3 is the key killer of apoptosis, thus promoting cell survival [23]. The value of the caspase 3 increased markedly in the HFD, HFruD and HFHF groups.

The caspases mechanism is negatively regulated by the BCL-2 family [1]. The BCL-2 family is classified into three subfamilies: a subfamily including BCL-2, a subfamily including Bax and Bak and a subfamily including Bik and Bid [37]. BCL-2 exerts anti-apoptotic activity by blocking a step which leads to the activation of caspases, while Bax exerts proapoptotic activity [37]. The ratio between anti-apoptotic and pro-apoptotic members of the BCL-2 family defines the liability of the cell to apoptosis [37]. As observed from our finding, non-significant changes occurred in BCL-2, while the value of Bax increased dramatically in all Western diet groups, especially in the HFHF group. Finally, the values of the BCL-2/Bax ratio decreased in all Western diet groups.

CONCLUSIONS

In conclusion, HFD, HFruD, and HFHF developed morphologic hepatic changes ranging from steatosis to necrosis and inflammation, besides the development of internal metabolic impairments. The chief factors of hepatic injury were fat accumulation in the hepatocytes, oxidative stress and highly elevated iNOS. Compared to the other groups, HFHF's effect was more prominent.

Ethical approval

All applicable international, national, and/or institutional guidelines for the care and use of animals were followed. The study was performed according to the ethical standards of the National Institutes of Health guide for the care and use of Laboratory Animals (NIH Publications No. 8023, revised 1978). The study was approved by the Ethics Committee, Faculty of Medicine, Cairo University (2433/2018).

REFERENCES

1. Adams JM, Cory S. The Bcl-2 protein family: arbiters of cell survival. Science. 1998; 281(5381): 1322–1326, indexed in Pubmed: 9735050.
2. Alberti KG, Eckel RH, Grundy SM, et al. Harmonizing the metabolic syndrome: a joint interim statement of the International Diabetes Federation Task Force on Epidemiology and Prevention; National Heart, Lung, and Blood Institute; American Heart Association; World Heart Federation; International Atherosclerosis Society; and International Association for the Study of Obesity. Circulation. 2009; 120(16): 1640–1645, doi: 10.1161/CIRCULATIONAHA.109.192644, indexed in Pubmed: 19805654.
3. Angulo P, Lindor KD. Non-alcoholic fatty liver disease. J Gastroenterol Hepatol. 2002; 17(Suppl): S186–S190.
4. Asakawa T, Yagi M, Tanaka Y, et al. The herbal medicine Inchinko-to reduces hepatic fibrosis in cholestatic rats. Pediatr Surg Int. 2012; 28(4): 379–384, doi: 10.1007/s00383-011-2974-5, indexed in Pubmed: 22045203.
5. Birben E, Sahiner U, Sackesen C, et al. Oxidative stress and antioxidant defense. World Allergy Organization J. 2012; 5(1): 9–19, doi: 10.1097/wox.0b013e3182439613.
6. Bocarsly ME, Powell ES, Avena NM, et al. High-fructose corn syrup causes characteristics of obesity in rats: increased body weight, body fat and triglyceride levels. Pharmacol Biochem Behav. 2010; 97(1): 101–106, doi: 10.1016/j.pbb.2010.02.012, indexed in Pubmed: 20219526.
7. Browning JD, Horton JD. Molecular mediators of hepatic steatosis and liver injury. J Clin Invest. 2004; 114(2): 147–152, doi: 10.1172/JCI22422, indexed in Pubmed: 15254578.
8. Collins S, Martin TL, Surwit RS, et al. Genetic vulnerability to diet-induced obesity in the C57BL/6J mouse: physiological and molecular characteristics. Physiol Behav. 2004; 81(2): 243–248, doi: 10.1016/j.physbeh.2004.02.006, indexed in Pubmed: 15159170.

9. Collison KS, Zaidi MZ, Saleh SM, et al. Effect of trans-fat, fructose and monosodium glutamate feeding on feline weight gain, adiposity, insulin sensitivity, adipokine and lipid profile. Br J Nutr. 2011; 106(2): 218–226, doi: 10.1017/S000711451000588X, indexed in Pubmed: 21429276.
10. Costa E, Rezende B, Cortes S, et al. Neuronal Nitric Oxide Synthase in Vascular Physiology and Diseases. Front Physiol. 2016; 7, doi: 10.3389/fphys.2016.00206.
11. Day CP, James OF. Hepatic steatosis: innocent bystander or guilty party? Hepatology. 1998; 27(6): 1463–1466, doi: 10.1002/hep.510270601, indexed in Pubmed: 9620314.
12. Day CP, James OF. Steatohepatitis: a tale of two "hits"? Gastroenterology. 1998; 114(4): 842–845, indexed in Pubmed: 9547102.
13. Dröge W. Free radicals in the physiological control of cell function. Physiol Rev. 2002; 82(1): 47–95, doi: 10.1152/physrev.00018.2001, indexed in Pubmed: 11773609.
14. Feldstein A, Gores G. Steatohepatitis and apoptosis: therapeutic implications. Am J Gastroenterol. 2004; 99(9): 1718–1719, doi: 10.1111/j.1572-0241.2004.40573.x.
15. Feldstein A, Canbay A, Angulo P, et al. Hepatocyte apoptosis and fas expression are prominent features of human nonalcoholic steatohepatitis. Gastroenterology. 2003; 125(2): 437–443, doi: 10.1016/s0016-5085(03)00907-7.
16. Folch J, Lees M, Sloane Stanley GH. A simple method for the isolation and purification of total lipides from animal tissues. J Biol Chem. 1957; 26(1): 497–509.
17. Ha SK, Chae C. Inducible nitric oxide distribution in the fatty liver of a mouse with high fat diet-induced obesity. Exp Anim. 2010; 59(5): 595–604, indexed in Pubmed: 21030787.
18. Hebbard L, George J. Animal models of nonalcoholic fatty liver disease. Nat Rev Gastroenterol Hepatol. 2011; 8(1): 35–44, doi: 10.1038/nrgastro.2010.191, indexed in Pubmed: 21119613.
19. Jurdak N, Lichtenstein AH, Kanarek RB. Diet-induced obesity and spatial cognition in young male rats. Nutr Neurosci. 2008; 11(2): 48–54, doi: 10.1179/147683008X301333, indexed in Pubmed: 18510803.
20. Larter CZ, Yeh MM. Animal models of NASH: getting both pathology and metabolic context right. J Gastroenterol Hepatol. 2008; 23(11): 1635–1648, doi: 10.1111/j.1440-1746.2008.05543.x, indexed in Pubmed: 18752564.
21. Lee JS, Jun DW, Kim EK, et al. Histologic and metabolic derangement in high-fat, high-fructose, and combination diet animal models. ScientificWorldJournal. 2015; 2015: 306326, doi: 10.1155/2015/306326, indexed in Pubmed: 26090514.
22. Li S, Liao X, Meng F, et al. Therapeutic role of ursolic acid on ameliorating hepatic steatosis and improving metabolic disorders in high-fat diet-induced non-alcoholic fatty liver disease rats. PLoS One. 2014; 9(1): e86724, doi: 10.1371/journal.pone.0086724, indexed in Pubmed: 24489777.
23. Ma J, Zou C, Guo L, et al. Novel Death Defying Domain in Met entraps the active site of caspase-3 and blocks apoptosis in hepatocytes. Hepatology. 2014; 59(5): 2010–2021, doi: 10.1002/hep.26769, indexed in Pubmed: 24122846.
24. Miele L, Valenza V, La Torre G, et al. Increased intestinal permeability and tight junction alterations in nonalcoholic fatty liver disease. Hepatology. 2009; 49(6): 1877–1887, doi: 10.1002/hep.22848, indexed in Pubmed: 19291785.
25. Pereira-Lancha LO, Campos-Ferraz PL, Lancha AH. Obesity: considerations about etiology, metabolism, and the use of experimental models. Diabetes Metab Syndr Obes. 2012; 5: 75–87, doi: 10.2147/DMSO.S25026, indexed in Pubmed: 22570558.
26. Peverill W, Powell LW, Skoien R. Evolving concepts in the pathogenesis of NASH: beyond steatosis and inflammation. Int J Mol Sci. 2014; 15(5): 8591–8638, doi: 10.3390/ijms15058591, indexed in Pubmed: 24830559.
27. Ribeiro PS, Cortez-Pinto H, Solá S, et al. Hepatocyte apoptosis, expression of death receptors, and activation of NF-kappaB in the liver of nonalcoholic and alcoholic steatohepatitis patients. Am J Gastroenterol. 2004; 99(9): 1708–1717, doi: 10.1111/j.1572-0241.2004.40009.x, indexed in Pubmed: 15330907.
28. Rolo AP, Teodoro JS, Palmeira CM. Role of oxidative stress in the pathogenesis of nonalcoholic steatohepatitis. Free Radic Biol Med. 2012; 52(1): 59–69, doi: 10.1016/j.freeradbiomed.2011.10.003, indexed in Pubmed: 22064361.
29. Schwartz DM, Wolins NE. A simple and rapid method to assay triacylglycerol in cells and tissues. J Lipid Res. 2007; 48(11): 2514–2520, doi: 10.1194/jlr.D700017-JLR200, indexed in Pubmed: 17717377.
30. Sheehan DC, Hrapchak BB. Theory and practice of histotechnology. 2d edn. Mosby, St Louis 1980.
31. Spruss A, Kanuri G, Wagnerberger S, et al. Toll-like receptor 4 is involved in the development of fructose-induced hepatic steatosis in mice. Hepatology. 2009; 50(4): 1094–1104, doi: 10.1002/hep.23122, indexed in Pubmed: 19637282.
32. Stark AH, Timar B, Madar Z. Adaptation of Sprague Dawley rats to long-term feeding of high fat or high fructose diets. Eur J Nutr. 2000; 39(5): 229–234, indexed in Pubmed: 11131370.
33. Takaki A, Kawai D, Yamamoto K. Multiple hits, including oxidative stress, as pathogenesis and treatment target in non-alcoholic steatohepatitis (NASH). Int J Mol Sci. 2013; 14(10): 20704–20728, doi: 10.3390/ijms141020704, indexed in Pubmed: 24132155.
34. Teli MR, James OF, Burt AD, et al. The natural history of nonalcoholic fatty liver: a follow-up study. Hepatology. 1995; 22(6): 1714–1719, indexed in Pubmed: 7489979.
35. Thornberry NA, Lazebnik Y. Caspases: enemies within. Science. 1998; 281(5381): 1312–1316, indexed in Pubmed: 9721091.
36. Tipple TE, Rogers LK. Methods for the determination of plasma or tissue glutathione levels. Methods Mol Biol. 2012; 889: 315–324, doi: 10.1007/978-1-61779-867-2_20, indexed in Pubmed: 22669674.
37. Tsujimoto Y. Role of Bcl-2 family proteins in apoptosis: apoptosomes or mitochondria? Genes to Cells. 1998; 3(11): 697–707, doi: 10.1046/j.1365-2443.1998.00223.x.
38. Wang MY, Grayburn P, Chen S, et al. Adipogenic capacity and the susceptibility to type 2 diabetes and metabolic syndrome. Proc Natl Acad Sci U S A. 2008; 105(16): 6139–6144, doi: 10.1073/pnas.0801981105, indexed in Pubmed: 18413598.
39. Wang Y, Ausman LM, Russell RM, et al. Increased apoptosis in high-fat diet-induced nonalcoholic steatohepatitis in rats is associated with c-Jun NH2-terminal kinase activation and elevated proapoptotic Bax. J Nutr. 2008; 138(10): 1866–1871, doi: 10.1093/jn/138.10.1866, indexed in Pubmed: 18806094.
40. Weydert CJ, Cullen JJ. Measurement of superoxide dismutase, catalase and glutathione peroxidase in cultured cells and tissue. Nat Protoc. 2010; 5(1): 51–66, doi: 10.1038/nprot.2009.197, indexed in Pubmed: 20057381.
41. Woodie L, Blythe S. The differential effects of high-fat and high-fructose diets on physiology and behavior in male rats. Nutr Neurosci. 2018; 21(5): 328–336, doi: 10.1080/1028415X.2017.1287834, indexed in Pubmed: 28195006.